Nuclear Inst. and Methods in Physics Research, A 958 (2020) 162037

Contents lists available at ScienceDirect

Nuclear Inst. and Methods in Physics Research, A

journal homepage: www.elsevier.com/locate/nima

Transition radiation measurements with a Si and a GaAs pixel sensor on a Timepix3 chip

F. Dachs [a,b,*], J. Alozy [a], N. Belyaev [c], B.L. Bergmann [d], M. van Beuzekom [e], T.R.V. Billoud [f], P. Burian [d,g], P. Broulim [g], M. Campbell [a], G. Chelkov [h], M. Cherry [i], S. Doronin [c], K. Filippov [c], P. Fusco [j,k], F. Gargano [k], B. van der Heijden [e], E.H.M. Heijne [a,d,e], S. Konovalov [l], X.L. Cudie [a], F. Loparco [j,k], V. Mascagna [m,n], M.N. Mazziotta [k], L. Meduna [d], H. Pernegger [a], D. Ponomarenko [c], S. Pospisil [d], M. Prest [m,n], C. Rembser [a], A. Romaniouk [c], A.A. Savchenko [c,o], D. Schaefer [p], E.J. Schioppa [a], D. Sergeeva [c,o], D. Shchukin [l], E. Shulga [c], S. Smirnov [c], Y. Smirnov [c], P. Smolyanskiy [h], M. Soldani [m,n], P. Spinelli [j,k], M. Strikhanov [c], P. Teterin [c], V. Tikhomirov [l], A.A. Tishchenko [c,o], E. Vallazza [q], K. Vorobev [c], K. Zhukov [l]

[a] CERN, Switzerland
[b] Technical University of Vienna, Austria
[c] National Research Nuclear University MEPhI, Russia
[d] Institute of Experimental and Applied Physics, Czech Technical University in Prague, Czech Republic
[e] Nikhef, The Netherlands
[f] Université de Montréal, Canada
[g] Faculty of Electrical Engineering, University of West Bohemia in Pilsen, Czech Republic
[h] Joint Institute for Nuclear Research, Russia
[i] Louisiana State University, United States
[j] INFN Bari, Italy
[k] Dipartimento di Fisica "M. Merlin" dell'Università e del Politecnico di Bari, Italy
[l] P. N. Lebedev Physical Institute of the Russian Academy of Sciences, Russia
[m] INFN Milano Bicocca, Italy
[n] Università degli Studi dell'Insubria, Como, Italy
[o] National Research Center Kurchatov Institute, Russia
[p] University of Chicago, United States
[q] INFN Trieste, Italy

A R T I C L E I N F O

Keywords:
Transition radiation
Timepix3
Gallium arsenide
Silicon

A B S T R A C T

Growing energies of particles at modern or planned particle accelerator experiments as well as cosmic ray experiments require particle identification at gamma-factors (γ) of up to $\sim 10^5$. At present there are no detectors capable of identifying charged particles with reliable efficiency in this range of γ. New developments in high granular pixel detectors allow one to perform simultaneous measurements of the energies and the emission angles of generated transition radiation (TR) X-rays and use the maximum available information to identify particles. First results of studies of TR energy-angular distributions using gallium arsenide (GaAs) sensors bonded to Timepix3 chips are presented. The results are compared with those obtained using a silicon (Si) sensor of the same thickness of 500 μm. The analysis techniques used for these experiments are discussed.

1. Introduction

Transition radiation (TR) is produced by a charged particle traversing an interface between two media with different dielectric constants. For ultra-relativistic particles, the energy of emitted photons extends into the X-ray region where the TR yield as a function of γ has a threshold character. This phenomenon is a basis for particle identification detectors. X-ray TR is peaked in a forward direction (within a few mrad) which makes it difficult to separate from the initial charged particle. Since the number of emitted TR photons per interface in this region is small (for typical detectors one per 20–30 interfaces) TR radiators consisting of multiple foils are usually built. Main characteristics of emitted TR are defined by the foil thickness l_1 and distances l_2 between foils. The X-ray TR emission threshold is defined by foil properties as $\gamma_{thr} \approx l_1 \omega_1 / c$, where ω_1 is the plasma frequency of the foil material.

* Correspondence to: Technical University of Vienna, Karlsplatz 13, 1040 Vienna, Austria.
E-mail addresses: florian.dachs@cern.ch, dachsf@gmail.com (F. Dachs).

https://doi.org/10.1016/j.nima.2019.03.092
Received 22 March 2019; Accepted 28 March 2019
Available online 1 April 2019

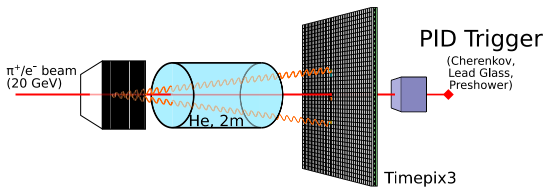

Fig. 1. Fluorescence calibration of a single pixel of the GaAs sensor.

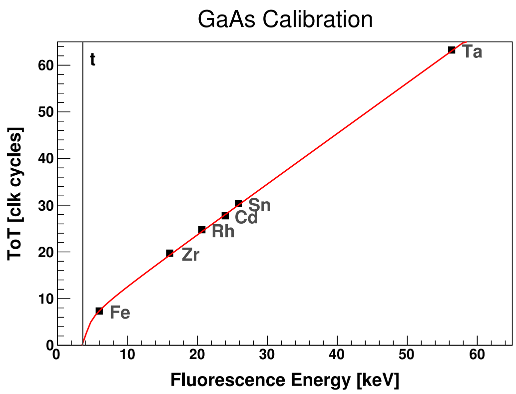

Fig. 2. Deposited energies of 20 GeV/c electrons and TR for Si and GaAs and cuts for beam particles.

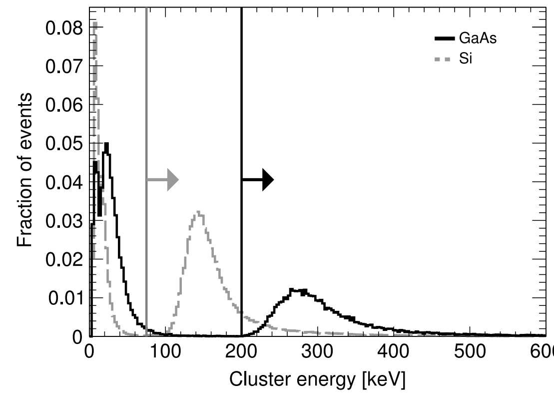

Fig. 3. A sketch of the test beam setup at the CERN SPS.

The distance between foils and the foil parameters are responsible for fine interference effects and for the TR yield saturation which happens at $\gamma_{sat} = 0.6\,\omega_1 \sqrt{l_1\, l_2}/c$ [1]. By changing the parameters of the radiator, the sensitivity of a TRD (Transition Radiation Detector) can be tuned to a certain γ-factor range (see for instance reviews [2,3]). This in turn makes TR attractive for particle identification at very high γ where other effects, such as Cherenkov radiation, reach saturation.

Most TRDs commonly operate at a range of $5 \times 10^2 < \gamma < 2 \times 10^3$ but with the increase of particle energies at modern or planned particle accelerator experiments as well as cosmic ray experiments particle identification (PID) at much higher γ-factors is required. For example, the proposal for a very forward spectrometer [4] at CERN would require hadron identification at γ-factors of up to $\gamma = 3.6 \times 10^4$. One of the ways to make such a kind of detector would be to use a multilayer radiator–detector structure with detectors where the particle ionization loss is less than the detected TR photon energy [5,6]. Another approach is based on fine granularity semiconductor detectors which would allow the simultaneous measurements of the TR photon energy and emission angle and maximize the available information to be used for particle identification [7]. In recent years the development of high resolution pixel chips such as Timepix3 [8] connected to thick Si or GaAs sensors opens new possibilities for high efficiency TR detectors with good spatial resolution of the charged particle and TR photons. First measurements of TR with a 500 μm Si-sensor attached to a Timepix3 chip were presented in [9]. In this paper, a comparison of the experimental results obtained with GaAs and Si sensors is presented.

2. Experimental setup

Studies were carried out at the CERN SPS facility with 20 GeV/c electrons and muons from 120 to 290 GeV/c using different types of radiators. The test beam set-up is shown schematically in Fig. 3.

It comprises:

- multi-foil radiators, which are made from 30 to 90 foils of equal thickness arranged at regular distances (a few mm). In this paper results for 30 Mylar foils of 50 μm thickness spaced out at regular intervals of 2.97 mm are presented. These Radiators were positioned at ∼ 2 m distance from the detector. A helium filled pipe was used in-between to prevent the absorption of emitted TR photons in air.
- a Timepix3 front-end bonded to either a Si or a chromium-compensated GaAs:Cr [10] sensor. The detector consists of a square matrix of 256 × 256 pixels at a pixel pitch of 55 μm, thus forming an active area of 1.98 cm^2. The sensor is 500 μm thick (for both materials) to maximize the TR detection efficiency. The "Katherine" interface was used to read information from the Timepix3 chip [11]. The Timepix3 chip was operated in data driven mode.
- a particle identification system (PID) consisting of an upstream Cherenkov counter (not shown), a preshower detector and a lead glass calorimeter. A hardware trigger related to the particle sort was used as a flag in the data stream.

Both Si and GaAs sensors were calibrated pixel by pixel using fluorescence lines of different elements. The calibration of a single pixel for GaAs is shown in Fig. 1. The calibration is limited to energies above ∼ 4.5 keV (GaAs) and ∼ 3 keV (Si) corresponding to the lowest threshold to be applied to minimize the number of triggers produced by noise hits. Below this energy, the calibration can only be done with test pulses which artificially produce signals in the Timepix3 front-end. The fit function is given by [12]:

$$ToT = a\,E + b - \frac{c}{E - t} \quad (1)$$

where a, b and c are fit parameters while t is the minimum threshold energy which can be detected. An essential property of the Timepix3 pixel readout is the recording of the time of incidence with 1.6 ns precision in each pixel. Using these time tags, it is easy to correlate the relevant TR photon conversions with the parent particle, by looking within a time window of a few 100 ns. The bias voltage applied to the sensors was −450 V for GaAs and −200 V for Si.

3. Data analysis

The trigger signals from the PID give a time stamp around which a time window is used to collect all fired pixels into an event. Within the event, pixels are clustered with an algorithm based on the telescope reconstruction software "Proteus" [13]. Pixels are grouped into a cluster if the following conditions for the pixel coordinates apply:

$$\Delta X = |X_i - X_j| \quad for\; i \neq j$$
$$\Delta Y = |Y_i - Y_j| \quad for\; i \neq j$$
$$(\Delta X = 1 \wedge \Delta Y = 0) \parallel (\Delta X = 0 \wedge \Delta Y = 1)$$

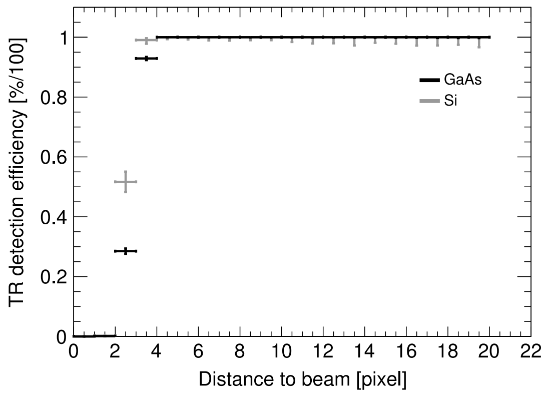

Fig. 4. Probability to recognize TR clusters at a certain distance from the beam cluster.

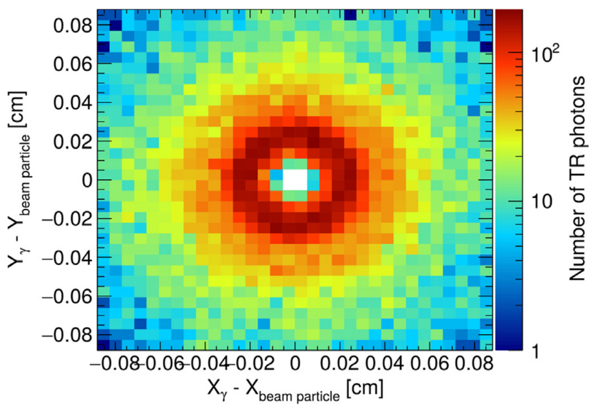

Fig. 5. Relative position of identified TR clusters relative to the beam (center).

Once all pixels have been grouped into clusters, cluster energies are calculated by simply summing up the energies of all its pixels. The cluster position is calculated as a center of gravity using the pixel energy ω as a weight:

$$\vec{x}_{COG} = (x_{COG}, y_{COG})^T = \frac{\sum_{j=0}^{clustersize} (x_i, y_j)^T \omega_j}{\sum_{j=0}^{clustersize} \omega_j} \tag{2}$$

The beam particle cluster is identified by choosing the cluster with the highest energy in the event. If that energy exceeds a given threshold (75 keV for Si, 200 keV for GaAs), the event is considered valid and analyzed. As shown in Fig. 2, the threshold energy is a sufficient cut to separate beam particle clusters from TR photon clusters. Subsequently, the number of secondary clusters and their distance to the beam particle cluster are calculated. From this information and geometry parameters of the experimental setup the emission angle and energy spectra of TR are obtained.

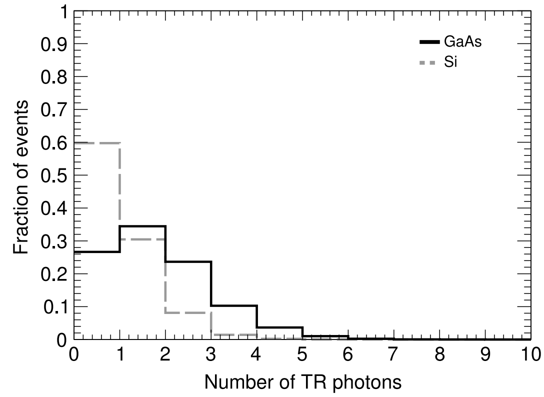

Fig. 6. Number of TR photons detected per event.

4. Results

A radial projection of the detector's ability to resolve TR and beam clusters is shown in Fig. 4. The probability to separate a TR cluster from the beam reaches 100% at a distance of 3 pixels which corresponds to 165 μm. This is mainly affected by the morphology of the beam particle clusters, which typically consist of 5 pixels, arranged in a cross-like shape. Thus, at a distance of 2 m to the radiator, this allows to detect TR photons produced at angles of down to 0.075 mRad. The distribution of TR photons around the beam can be seen in Fig. 5.

The multiplicity distribution of detected TR photons per particle for Si and GaAs sensors is shown in Fig. 6. One sees that for the same radiator the number of detected photons with GaAs detectors is larger than that of the Si detector.

Energy-angular distributions of the detected transition radiation photons for both detectors are shown in Figs. 7(a) and 7(b). These figures clearly show the global and fine interference structure of TR. One sees that the GaAs detector is much more effective for high energy TR photons. Projections of these distributions on the energy axis are shown in Fig. 8(a). One clearly sees that for the soft part of the spectrum (up to ~13 keV) both detectors have good efficiency. However if TR photons have energies above 20 keV GaAs detectors are much more

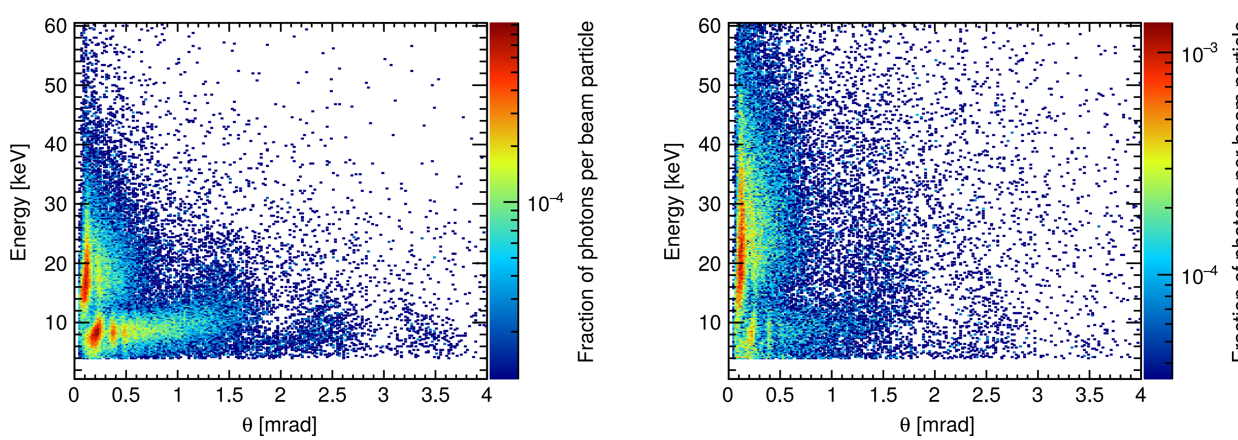

(a) Energy over angle of TR measured with a Si sensor.
(b) Energy over angle of TR measured with a GaAs sensor.

Fig. 7. Energy and angle spectra measured with Si and GaAs sensors.

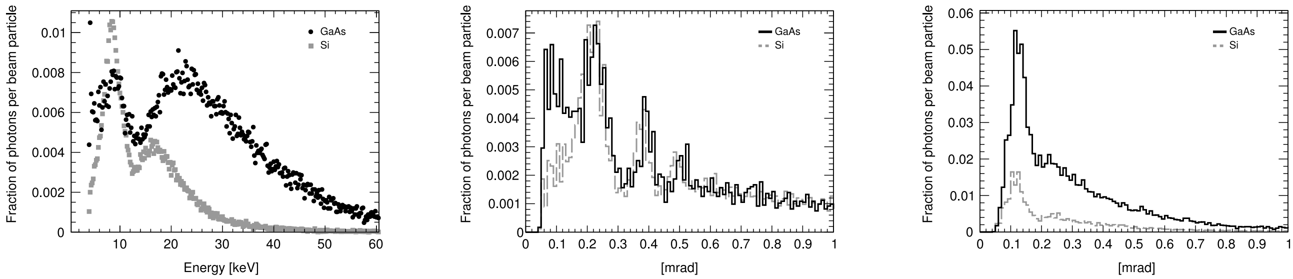

(a) Energy spectra measured with Si and GaAs sensors.

(b) Angular distribution of TR measured with Si and GaAs sensors for photon energies < 13 keV. The cause for the small-angle peak for GaAs data may be related to fluorescence photons escaping the particle clusters.

(c) Angular distribution of TR measured with Si and GaAs sensors for photon energies >13 keV.

Fig. 8. Projected angular and energy distributions measured with Si and GaAs sensors.

effective. The angular distributions show multiple peaks (Fig. 8(b) and Fig. 8(c)) due to interference between foils. There is good agreement of data for the two sensor materials in the low energy region except for very small angles. The origin of this discrepancy is not yet entirely clear but most likely fluorescence photons emitted from the beam clusters are a part of the effect.

5. Conclusions

The recently developed Timepix3 pixel front-end attached to a high quality GaAs sensor makes an efficient X-ray detector with high spatial resolution and good energy resolution possible. This offers a possibility to detect X-ray transition radiation photons and separate them from the particle ionization clusters. Energies and emission angles of TR can be measured simultaneously which allows to enhance the particle identification performance of TRDs based on this technology. A comparison of first results of the test beam measurements performed in 2017 (Si sensor) and 2018 (GaAs sensor) shows that angular and energy measurement parameters of these two detectors are in good agreement at energies below 13 keV. However, if TR photons have energies above 20 keV GaAs detectors are the most efficient ones.

Acknowledgments

We gratefully acknowledge the financial support from Russian Science Foundation grant (project No. 16-12-10277).

The work was supported from European Regional Development Fund-Project “Van de Graaff Accelerator - a Tunable Source of Monoenergetic Neutrons and Light Ions” (No. CZ.02.1.01/0.0/0.0/16_013/0001785).

References

[1] M.L. Cherry, Measurements of the spectrum and energy dependence of x-ray transition radiation, Phys. Rev. D 17 (1978) 2245–2260.

[2] B. Dolgoshein, Transition radiation detectors, Nucl. Instrum. Methods A 326 (3) (1993) 434–469.

[3] A. Andronic, et al., Transition radiation detectors, Nucl. Instrum. Methods A 666 (2011) 130–174.

[4] M. Albrow, A very forward hadron spectrometer for the LHC and cosmic ray physics, Proc. Sci. (2018) PoS(EDSU2018).

[5] A. Romaniouk, Progress in TRD for identifying multi-TeV hadrons, 2017, Cross sections for Cosmic Rays @ CERN.

[6] N. Belyaev, et al., Test beam studies of possibilities to separate particles with gamma factors above 10^3 with straw based transition radiation detector, J. Phys. Conf. ser. 934 (2018) 012053, (2018).

[7] J. Alozy, et al., Identification of particles with lorentz factor up to 10^4 with transition radiation detectors based on micro-strip silicon detectors, Nucl. Instrum. Methods A 927 (2019) 1–13, in print, arXiv:1901.11265.

[8] T. Poikela, et al., Timepix3: a 65K channel hybrid pixel readout chip with simultaneous ToA/ToT and sparse readout, J. Instrum. 9 (05) (2014) C05013–C05013.

[9] E.J. Schioppa, et al., First measurements of the spectral and angular distribution of transition radiation using a silicon pixel sensor on a Timepix3 chip, Nucl. Instrum. Methods A (2018) in print.

[10] P. Smolyanskiy, et al., Properties of GaAs: Cr-based Timepix detectors, J. Instrum. 13 (02) (2018) T02005–T02005.

[11] P. Burian, et al., Katherine: Ethernet embedded readout interface for Timepix3, J. Instrum. 12 (11) (2017) C11001–C11001.

[12] J. Jakubek, Precise energy calibration of pixel detector working in time-over-threshold mode, Nucl. Instrum. Methods A 633 (2011) S262 – S266, 11th International Workshop on Radiation Imaging Detectors (IWORID).

[13] M. Kiehn, et al., Proteus beam telescope reconstruction, 2019, http://dx.doi.org/10.5281/zenodo.2579153.